Research Article

Improvement of 3D Printing Elongation Using a Continuous Vibrator Device

Laongdaw Techawinyutham and Thanapat Sangkharat*
Department of Production and Robotics Engineering, Faculty of Engineering, King Mongkut's University of Technology North Bangkok, Bangkok, Thailand

* Corresponding author. E-mail: thanapat.s@eng.kmutnb.ac.th DOI: 10.14416/j.asep.2025.05.004
Received: 26 January 2025; Revised: 16 February 2025; Accepted: 10 March 2025; Published online: 21 May 2025

Abstract
3D printing is increasingly used in various industries due to its ability to easily fabricate complex shape parts. However, the low mechanical properties of 3D-printed parts remain a major drawback. Numerous studies have focused on enhancing mechanical properties through material improvements, process optimization, and high-strength reinforcement materials. However, limited research has explored the effect of continuous vibration on interlayer bonding and mechanical properties, an area that remains largely unstudied. A vibration device was attached to the printer base, generating vibration during the printing process. Dog-bone-shaped workpieces were printed in horizontal (x-y plane) and vertical (z-axis) orientations using three vibration frequencies: 50 Hz, 77 Hz, and 105 Hz, with a fixed amplitude of 0.03 mm. The results revealed that vibration improved interlayer bonding and the elongation of samples but had no significant effect on tensile strength, while surface roughness was slightly poorer compared to non-vibrated samples. At 50 Hz, elongation increased by 62.7% for horizontal workpieces and 21.6% for vertical ones. Similarly, at 77 Hz and 105 Hz, elongation improvements were 95.2% and 98.1% for horizontal workpieces, and 20.1% and 22.8% for vertical ones, respectively. Optical microscopy analysis showed that the enhanced elongation was due to increased interlayer adhesion, as the vibration facilitated material insertion between layers.

Keywords: 3D printing, Additive manufacturing, Fused deposition modeling, Interlayer, Vibration

1 Introduction

Recently, novel manufacturing processes have focused on minimizing material waste, production costs, and time. As a result, manufacturing methods with minimal material waste, such as Additive Manufacturing (AM) and metal spinning, have gained significant interest in modern production. One widely used AM technique is 3D printing. The advantages of 3D printing technology are flexible processing, the ability to create complex shapes, and low material waste. This technology is widely applied in many industries. However, the low mechanical properties of 3D-printed parts remain a limitation. As a result, this method is often used primarily for building prototypes. Improving the mechanical properties of 3D-printed workpieces remains a significant challenge in 3D printing research. This is especially true for technologies like fused deposition modeling (FDM) and direct ink writing (DIW), which are commonly used for 3D printing. Both processes are known for their weak interlayer strength [1]–[3]. Consequently, extensive research has been conducted to enhance interlayer strength. Improving the 3D printing path is one of the methods to enhance the mechanical properties of 3D-printed workpieces. There are two main types of paths: the contour-parallel path and the parallel-scan path [4]. The contour-parallel path involves the printer head moving along the shape of the workpiece, typically used for creating the outer shape of the workpiece with high precision. The parallel-scan path, on the other hand, is primarily used for building the internal material of the workpiece and plays a significant role in determining its properties. Most commercial 3D printers use a combination of these two paths, a technique referred to as a hybrid toolpath. Several studies have focused on optimizing the parallel-scan path to improve the performance of

the 3D printing process [5], [6]. However, standard parallel-scan paths are commonly used in research to study the mechanical properties of 3D-printed workpieces [7]–[12].

Numerous studies have focused on improving the mechanical properties of 3D-printed workpieces. Methods such as incorporating nanoparticles [13], fibers [14], and applying heat treatment [15] have been widely explored. Optimizing process parameters is another area of significant research. Parameters studied include nozzle temperature, nozzle movement speed, nozzle size, material infill percentage, and heat bed temperature [16], [17]. However, the addition of carbon fiber and optimizing process parameters cannot significantly enhance interlayer mechanical properties [18].

The weakest aspect of 3D-printed workpieces lies in the interlayer direction, where tensile strength is reduced by 10–65% compared to the printing direction. This reduction occurs because of poor bonding strength between layers [19]. As a result, optimizing infill and patterns has minimal impact on this strength. Instead, the strength between layers is primarily influenced by thermal transfer during printing, which affects the microstructures formed between layers [20], [21]. The formation of polymer chains occurs in three stages: wetting, diffusion, and randomization. These stages significantly impact the microstructure and, consequently, the interlayer strength of the workpiece. Additionally, studies have shown that increasing the heating time at critical temperatures can enhance interlayer bond strength, further improving the mechanical properties of 3D-printed workpieces in the interlayer direction [22], [23]. Several techniques have been developed to enhance the strength of interlayer bonds in the FDM process. These include post-processing heat treatments and applying heat during printing to improve material transfer at the contact points by increasing the temperature. Methods such as infrared and laser heating have been employed to raise the surface temperature of the workpiece, thereby improving adhesion at the interlayer interfaces [24], [25]. Additionally, ultrasonic vibration has been introduced during the printing process to enhance polymer distribution at contact points. This approach has proven effective in strengthening interlayer bonds and improving the isotropy and overall strength of FDM-printed parts [19]. Several methods have been explored to enhance interlayer strength, as mentioned above. However, vibration has not yet been applied to improve interlayer bonding.

Vibration during the 3D printing process has primarily been studied for its impact on reducing 3D-printed workpiece quality. These vibrations typically arise from the rapid movement of the print bed or print head, followed by abrupt stops, which can negatively affect the shape and surface quality of the printed workpiece. Mishra *et al.* [26] investigated the vibration of three 3D printer models at frequencies ranging from 200 Hz to 1 kHz. Their study demonstrated the effects of vibration frequency on part quality and showed that frequency can be used to assess printer conditions. Additionally, Kam *et al.* [27] found that printing direction influences machine vibration and the properties of the workpiece. However, vibrations may also have a beneficial effect by enhancing material transfer between interlayers, thereby increasing interlayer bond strength—a promising aspect that remains underexplored. Tofangchi *et al.* [19] applied ultrasonic vibrations at 34.4 kHz during the printing process. This vibration increased adhesion strength between layers by 10%.

This study explores a novel application of vibration in 3D printing by incorporating a vibrating motor on the printer base and conducting experiments with workpieces printed in both horizontal (x-y plane) and vertical (z-axis) orientations. This study utilized continuous sub-ultrasonic frequencies (50–105 Hz). The introduction of vibration enhanced material transfer between interlayers, resulting in a significant improvement in the workpiece's mechanical properties, particularly its toughness, without notably affecting its tensile strength.

2 Materials and Method

2.1 *Materials*

2.1.1 3D printing machine

The Mini 2ES series printer from the UP company was used in this study. The 3D printing process for this study was conducted with specific parameters to ensure consistent quality in the workpieces. A nozzle size of 0.4 mm and a layer height of 0.25 mm were used, with a rectilinear infill pattern set at 80% density to provide structural integrity. A workpiece with 80% infill density has sufficient strength for tensile testing in both horizontal and vertical printing directions. Additionally, it requires less material and time compared to 100% infill. The heat bed temperature was maintained at 90 °C to enhance layer adhesion, while the printing temperature was set at 270 °C to

ensure optimal material flow and bonding. This study aims to examine the effect of vibration, the printing parameters were kept constant for all experiments. An acrylonitrile butadiene styrene (ABS) filament with a diameter of 1.75 mm was used in the experiments. The filament is the X3D ABS model, manufactured by the same brand as the 3D printer, with a density of 1.05 g/cm³, a tensile strength of 46 MPa, and a tensile elongation of 25%.

2.1.2 Vibration equipment

The vibration device was constructed using a 12-volt DC motor and unbalanced weights. Two ballast weights, each with a diameter of 10 mm, a thickness of 5 mm, and a weight of 0.3 g, were attached to both sides of the motor axis. These weights were positioned off-center to generate vibrations during motor rotation. The vibration frequency was adjustable by varying the motor's power supply voltage. The vibrator was mounted on the 3D printer base, and its frequency and amplitude were measured using a vibration transmitter. A PCB Piezotronics Series 352C33 vibration sensor was installed on the printer base to monitor vibrations. NI cDAQ-9171 DAQ series was used to capture the signal from the vibration sensor. The sensor's output was transmitted to LABVIEW software for precise frequency and amplitude measurements. The experimental setup, depicted in Figure 1, was designed to test vibration frequencies of 50, 77, and 105 Hz, with a fixed amplitude of 0.03 mm. The maximum frequency of 105 Hz was chosen because it is the highest vibration frequency the 3D printer's base can withstand. Using a higher frequency would generate excessive vibration, potentially damaging the base. Conversely, frequencies below 50 Hz would be insufficient to induce noticeable vibration in the printer's base.

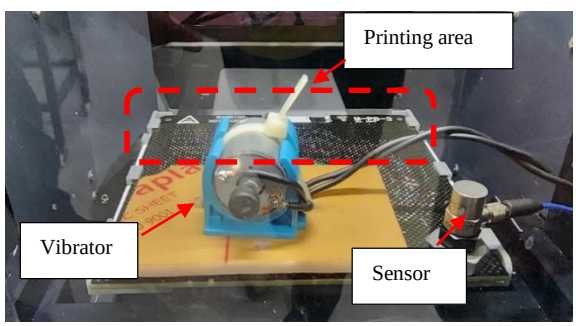

Figure 1: Installation of the vibrator and sensor in the 3D printer base.

2.2 *Experiments*

This study conducted experiments using two printing orientations: horizontal (x-y plane) and vertical (z-axis). The workpieces were designed according to the ASTM D638 standard and printed using a 3D printer equipped with an installed vibrator. The vibrator was activated and remained operational throughout the entire printing process to evaluate its effect on the mechanical properties of the workpieces. Three vibration frequencies were applied: 50 Hz, 77 Hz, and 105 Hz, with a fixed amplitude of 0.03 mm.

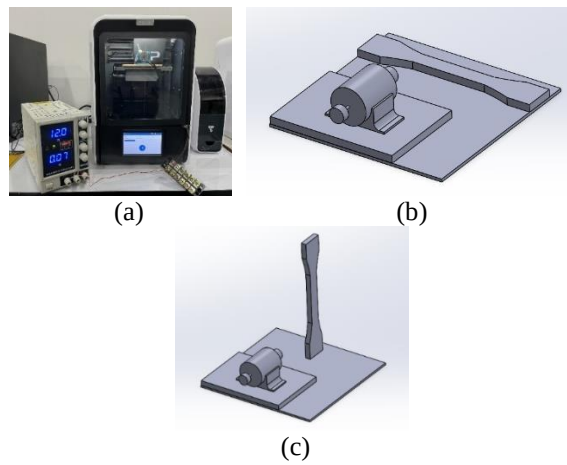

Figure 2: Photos of (a) the printing process, (b) horizontal printing orientation, and (c) vertical printing orientations of the workpiece.

In the experiment, the first five layers were printed without activating the vibration equipment to prevent the nozzle head from colliding with the printer bed and causing potential damage. From the sixth layer onward, the vibration equipment was operated at different vibration frequencies, which were adjusted by varying the voltage supplied to the motor. The experiment involved printing dog-bone-shaped samples in both horizontal (x-y plane) and vertical (z-axis) orientations, as illustrated in Figure 2, with three samples printed for each printing orientation. After the printing process, the dog-bone samples were tested for tensile strength and surface flatness to evaluate the effects of vibration on their properties.

2.2.1 Morphology testing

The traditional VMM (video measuring machine) "CHOTEN series SP3020" was used for examination

to assess the arrangement and interaction of each layer.

2.2.2 *Surface roughness measurement*

Surface roughness measurements were carried out using an Accretech Surfcom Touch 50 machine. The roughness of both the sides and the top of the workpieces was assessed prior to tensile testing. The measurements adhered to the JIS2001/2013 standard, with an evaluation length of 10.00 mm and a measurement speed of 0.3 mm/s. The procedure for measuring the top and side surface roughness is illustrated in Figure 3.

(a) (b)

Figure 3: Surface roughness measurement at (a) side surface and (b) top surface.

2.2.3 *Tensile testing*

Tensile testing was performed using an Instron 5566 universal testing machine at a constant speed of 10 mm/min. The tests were conducted at room temperature, and each workpiece was pulled until it fractured. The experiments were repeated three times for consistency. Following the tensile tests, the fractured workpieces were analyzed through both visual inspection and microscopic examination to assess the failure characteristics.

3 Results and Discussion

3.1 *External characteristics*

From Figure 4(a)–(f), the fracture patterns of workpieces subjected to vibration at different frequencies exhibit noticeable differences compared to those printed without vibration. Workpieces printed with vibration exhibit a more ductile fracture, as indicated by wider separation zones compared to workpieces printed without vibration (Figure 4(a)), due to reduced bonding distance before fracture. The larger separation zones were observed at 77 Hz (Figure 4(c)), followed by 105 Hz and 50 Hz. This improvement was due to increased intermixing with frequency [19]. Therefore, 50 Hz did not provide sufficient intermixing. The wider separation zones in the vibrated samples highlight improved interlayer bonding, contributing to the increased ductility of the workpieces [27].

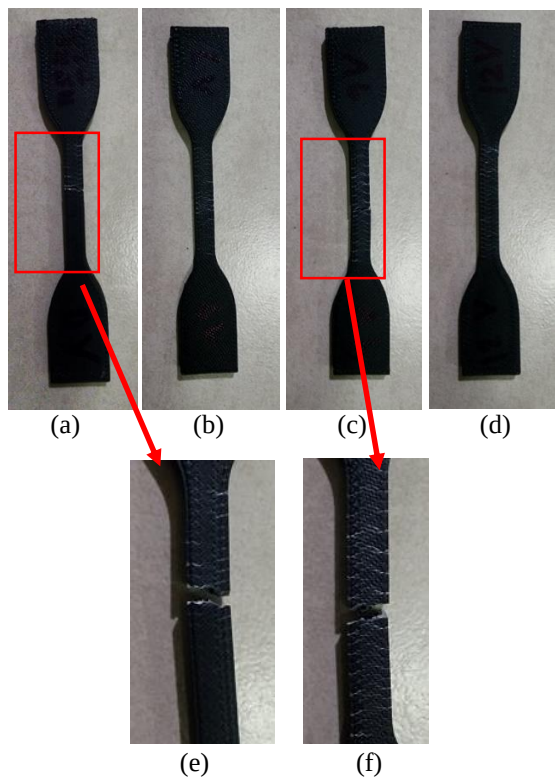

(a) (b) (c) (d)

(e) (f)

Figure 4: The workpieces after the tensile test: (a) without vibration, and with vibration during printing at frequencies of (b) 50 Hz, (c) 77 Hz, and (d) 105 Hz, and the surface areas in (e) no vibration and 77 Hz vibration.

Figure 5 illustrates the side surface of the workpieces before the tensile test. For the workpieces printed without vibration, the layers are arranged linearly, with no observable intermingling of material between layers. In contrast, when vibration is applied during printing, material from adjacent layers intermixes, resulting in a non-linear layer arrangement visible to the naked eye. Additionally, as the vibration frequency increases, the degree of material intermixing between layers becomes more prominent.

This intermixing also be confirmed by microscope images. The vibration at 77 Hz produced the largest intermingling zones, followed by 105 Hz and 50 Hz, showing a similar trend to the tensile fracture surface results. The increased intermixing enhances the toughness of the workpiece. This finding aligns with the experiment by Tofangchi *et al.*, [19], who used ultrasonic vibration frequencies. They attributed the increased intermixing to ultrasound-induced enhancement of polymer chain relaxation through secondary interactions.

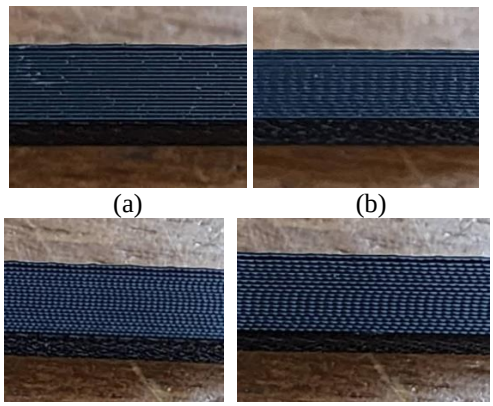

(a) (b) (c) (d)

Figure 5: Side surface of the workpiece: (a) without vibration, and with vibration at frequencies of (b) 50 Hz, (c) 77 Hz, and (d) 105 Hz.

Figure 6 illustrates the top surface of the workpieces. When observed with the naked eye, the workpieces printed without vibration exhibit a smooth and orderly pattern. In contrast, the workpieces printed with vibration display a wave-like surface appearance, reflecting the influence of the applied vibration on the printing process.

(a) (b) (c) (d)

Figure 6: Top surface of the workpiece under different vibrations: (a) no vibration, (b) 50 Hz, (c) 77 Hz, and (d) 105 Hz.

Figure 7 displays microscope images of the side surface of the workpieces at 10x magnification. In the workpieces printed without vibration, there is no visible intermixing of material between the layers. However, for the workpieces printed with vibration at 105 Hz, material intermixing between layers is evident. This intermingling of material between layers contributes to enhancing the strength of the interlayer adhesion [28].

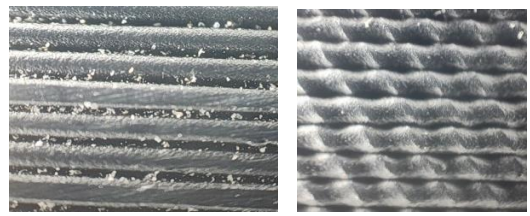

(a) (b)

Figure 7: OM images at 10x magnification: (a) without vibration and (b) with 105 Hz vibration.

3.2 *Surface roughness results*

The surface roughness results are presented in Figure 8, measured using Pt values, which represent the peak-to-valley profile height. The side surface roughness values ranged from 72.94 to 96.63 µm, while the top surface roughness values ranged from 61.07 to 131.17 µm. The maximum Pt value was observed in the workpiece subjected to 77 Hz vibration. In summary, vibration influences surface roughness, consistent with the findings of Kam *et al.*, [27]. Related research noted that vibration influenced the workpiece's surface roughness, tensile strength, and elongation.

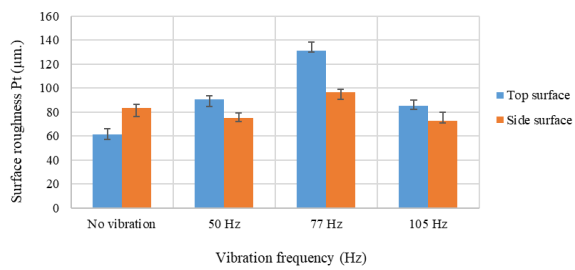

Figure 8: Surface roughness measurements from the top and side surfaces.

3.3 *Tensile testing results*

The tensile test was conducted on workpieces printed in two orientations: horizontal, as shown in Figure 2(b), and vertical, as shown in Figure 2(c). The tensile test results for the horizontal direction are presented in Figure 9. Vibration has a substantial impact on the mechanical properties of printed parts [27]. The

results revealed that the workpiece printed without vibration exhibited the lowest elongation before failure, breaking at a distance of 4.77 mm with a maximum tensile strength of 24.16 MPa. When vibration at a frequency of 50 Hz and an amplitude of 0.03 mm was applied, the elongation increased to 7.76 mm (a 62.7% improvement), with a maximum tensile strength of 25.49 MPa. Further increasing the vibration frequency to 77 Hz and 105 Hz resulted in elongations of 9.31 mm and 9.45 mm, corresponding to improvements of 95.2% and 98.1%, respectively, with maximum tensile strengths of 22.01 MPa and 21.56 MPa, respectively.

The increased elongation is attributed to enhanced interlayer bonding due to vibration, which improves the strength between layers [29]. This observation was also reported by Shunmugam *et al*., [30], who found that a lower printing speed improved mechanical properties due to enhanced interlayer bonding. However, the maximum tensile strength varied, showing both increases and decreases. This variation is hypothesized to be due to non-linear and discontinuous filament paths caused by interlayer material insertion during vibration, potentially affecting load distribution and thus influencing the maximum tensile strength. When comparing the workpieces with and without vibration, as shown in Figure 7, it was found that the workpiece without vibration had straight filament lines, while the workpiece with vibration had filament lines resembling a sine wave. When a force was applied, the sine-wave-shaped filament could stretch further, resulting in a higher elongation value for the workpiece. However, at the same time, the sine-wave-shaped filament could withstand less tensile force compared to the straight filament because it experienced bonding earlier. This can be observed from the tensile test graph, where the maximum tensile strength of the workpiece with vibration occurred at a higher stroke distance than that of the workpiece without vibration. For example, the maximum tensile strength of the workpiece without vibration occurred at a stroke of 3.54 mm, while the workpiece with 105 Hz vibration occurred at a stroke of 3.92 mm.

Figure 10 presents the tensile test results for workpieces printed in the vertical orientation. The results indicated that the workpiece printed without vibration broke at an elongation of 4.03 mm, with a maximum tensile strength of 13.67 MPa. When vibration was introduced at a frequency of 50 Hz with an amplitude of 0.03 mm, the elongation increased to 4.9 mm (a 21.6% improvement), with a maximum tensile strength of 14.61 MPa. Increasing the vibration frequency to 77 Hz and 105 Hz resulted in elongations of 4.84 mm and 4.95 mm, corresponding to improvements of 20.1% and 22.82%, respectively. The maximum tensile strengths for these frequencies were recorded as 19.43 MPa and 14.61 MPa, respectively. In a similar manner to horizontal workpieces, vibration causes material intermixing between layers, which results in an increase in elongation [19]. Moreover, strong interlayer bonding enhances the mechanical strength of the printed parts [31].

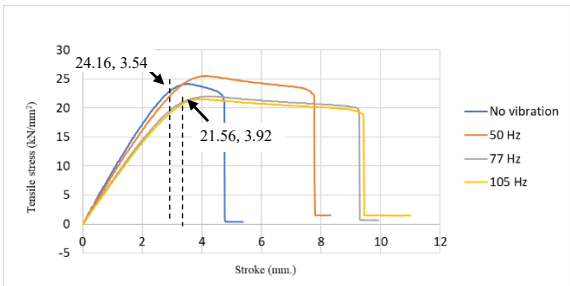

Figure 9: Tensile results of workpieces printed in the horizontal direction.

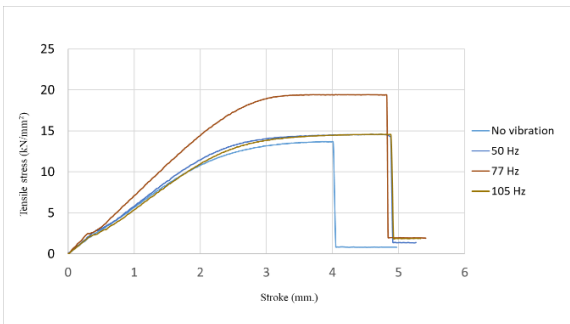

Figure 10: Tensile results of workpieces printed in the vertical direction.

4 Conclusions

The experimental results indicate that the maximum tensile strength of horizontally printed workpieces without vibration is slightly lower than the typical tensile strength range of ABS material (29.6–48 MPa), aligning with findings from prior research on tensile testing of 3D-printed ABS workpieces. Additionally, the maximum tensile strength of vertically printed workpieces is 43.4% lower compared to horizontally printed workpieces. This reduction is attributed to the lower interlayer bonding strength inherent in 3D-

printed structures, consistent with observations reported in related studies.

Base vibration promotes material interlayer bonding, enhancing the workpiece's toughness and elongation both horizontally and vertically direction. Horizontally printed workpieces with vibration exhibited maximum tensile strength comparable to those without vibration. A significant increase in elongation before failure was observed, with 105 Hz vibration achieving 9.45 mm elongation with an improvement of 98.1%. A vibration frequency of 50 Hz is recommended to enhance the elongation and tensile strength of workpieces. In vertically printed workpieces, the maximum tensile strength was comparable to non-vibrated workpieces, except at 77 Hz, where it reached 19.43 MPa with a 42.1% increase. The highest elongation before failure was at 105 Hz (4.95 mm), increasing 22.82%. Similar to horizontally printed workpieces, this improvement is attributed to enhanced interlayer bonding. Vibration frequencies of 77 Hz and 105 Hz are recommended to enhance the elongation and tensile strength of workpieces.

Acknowledgments

This research was funded by Science and Technology Research Institute, King Mongkut's University of Technology North Bangkok with contract no. KMUTNB-68-BASIC-50.

Author Contributions

L.T.: conceptualization, data analysis, writing an original draft, writing reviewing and editing; T.S.: conceptualization, research design, investigation, methodology, data analysis, writing an original draft, writing reviewing and editing. All authors have read and agreed to the published version of the manuscript.

Conflicts of Interest

The authors declare no conflict of interest.

References

[1] J. Liu, A. T. Gaynor, S. Chen, Z. Kang, K. Suresh, A. Takezawa, L. Li, J. Kato, J. Tang, C. C. L. Wang, L. Cheng, X. Liang, and A. C. To, "Current and future trends in topology optimization for additive manufacturing," *Structural and Multidisciplinary Optimization*, vol. 57, no. 6, pp. 2457–2483, Jun. 2018, doi: 10.1007/s00158-018-1994-3.

[2] A. Garg and A. Bhattacharya, "An insight to the failure of FDM parts under tensile loading: finite element analysis and experimental study," *International Journal of Mechanical Sciences*, vol. 120, pp. 225–236, Jan. 2017, doi: 10.1016/j.ijmecsci.2016.11.032.

[3] P. Zhang, J. Liu, and A. C. To, "Role of anisotropic properties on topology optimization of additive manufactured load bearing structures," *Scripta Materialia*, vol. 135, pp. 148–152, Jul. 2017, doi: 10.1016/j.scriptamat.2016.10.021.

[4] K.-M. M. Tam and C. T. Mueller, "Additive manufacturing along principal stress lines," *3D Printing and Additive Manufacturing*, vol. 4, no. 2, pp. 63–81, Jun. 2017, doi: 10.1089/3dp.2017.0001.

[5] A. Dogru, A. Sozen, G. Neser, and M. O. Seydibeyoglu, "Effects of aging and infill pattern on mechanical properties of hemp reinforced PLA composite produced by fused filament fabrication (FFF)," *Applied Science and Engineering Progress*, vol. 14, no. 4, pp. 651–660, 2021, doi: 10.14416/j.asep.2021.08.007

[6] Y. Jin, Y. He, G. Xue, and J. Fu, "A parallel-based path generation method for fused deposition modeling," *The International Journal of Advanced Manufacturing Technology*, vol. 77, no. 5–8, pp. 927–937, Mar. 2015, doi: 10.1007/s00170-014-6530-z.

[7] S. R. Rajpurohit and H. K. Dave, "Analysis of tensile strength of a fused filament fabricated PLA part using an open-source 3D printer," *The International Journal of Advanced Manufacturing Technology*, vol. 101, no. 5–8, pp. 1525–1536, Apr. 2019, doi: 10.1007/s00170-018-3047-x.

[8] A. Dhandapani, S. Krishnasamy, R. Nagarajan, S. M. K. Thiagamani, and C. Muthukumar, "Study on the inter-laminar shear strength and contact angle of glass fiber/ABS and glass fiber/carbon fiber/ABS hybrid composites," *Applied Science and Engineering Progress*, vol. 16, no. 3, 2023, doi: 10.14416/j.asep.2023.02.004.

[9] F. S. Shahar, M. T. H. Sultan, A. U. M. Shah, S. N. A. Safri, "A comparative analysis between conventional manufacturing and additive manufacturing of ankle-foot orthosis," *Applied Science and Engineering Progress*, vol. 13, no. 2, 2020, doi: 10.14416/j.asep.2020.03.002.

[10] R. J. Zaldivar, D. B. Witkin, T. McLouth, D. N. Patel, K. Schmitt, and J. P. Nokes, "Influence of processing and orientation print effects on the mechanical and thermal behavior of 3D-printed ULTEM® 9085 material," *Additive Manufacturing*, vol. 13, pp. 71–80, Jan. 2017, doi: 10.1016/j.addma.2016.11.007.

[11] Y. Song, Y. Li, W. Song, K. Yee, K.-Y. Lee, and V. L. Tagarielli, "Measurements of the mechanical response of unidirectional 3D-printed PLA," *Materials & Design*, vol. 123, pp. 154–164, Jun. 2017, doi: 10.1016/j.matdes. 2017.03.051.

[12] S. Ravindrababu, Y. Govdeli, Z. W. Wong, and E. Kayacan, "Evaluation of the influence of build and print orientations of unmanned aerial vehicle parts fabricated using fused deposition modeling process," *Journal of Manufacturing Processes*, vol. 34, pp. 659–666, Aug. 2018, doi: 10.1016/j.jmapro.2018.07.007.

[13] A. Dulaj, S. Peeters, P. Poorsolhjouy, T. A. M. Salet, and S. S. Lucas, "Combined analytical and numerical modelling of the electrical conductivity of 3D printed carbon nanotube-cementitious nanocomposites," *Materials & Design*, vol. 246, Oct. 2024, Art. no. 113324, doi: 10.1016/j.matdes.2024.113324.

[14] A. Pandian and S. Jailani, "Development and investigation of jute/linen fibre reinforced polymer composite," in *the International Conference on Advances in Design, Materials, Manufacturing and Surface Engineering for Mobility*, 2019, pp. 2019-28–0171, doi: 10.4271/ 2019-28-0171.

[15] Z. Weng, J. Wang, T. Senthil, and L. Wu, "Mechanical and thermal properties of ABS/montmorillonite nanocomposites for fused deposition modeling 3D printing," *Materials & Design*, vol. 102, pp. 276–283, Jul. 2016, doi: 10.1016/j.matdes.2016.04.045.

[16] Z. Guo, Z. Hou, X. Tian, W. Zhu, C. Wang, M. Luo, A. V. Malakhov, A. N. Polilov, D. Zhi, H. Ding, and H. Lan, "3D printing of curvilinear fiber reinforced variable stiffness composite structures: A review," *Composites Part B: Engineering*, vol. 291, Art. no. 112039, Feb. 2025, doi: 10.1016/j.compositesb.2024.112039.

[17] Y. Alex, N. C. Divakaran, I. Pattanayak, B. Lakshyajit, P. V. Ajay, and S. Mohanty, "Comprehensive study of PLA material extrusion 3D printing optimization and its comparison with PLA injection molding through life cycle assessment," *Sustainable Materials and Technologies*, vol. 43, Apr. 2025, Art. no. e01222, doi: 10.1016/j.susmat.2024.e01222.

[18] R. A. Wach, P. Wolszczak, and A. Adamus-Wlodarczyk, "Enhancement of mechanical properties of FDM-PLA parts via thermal annealing," *Macromolecular Materials and Engineering*, vol. 303, no. 9, Sep. 2018, Art. no. 1800169, doi: 10.1002/mame.201800169.

[19] A. Tofangchi, P. Han, J. Izquierdo, A. Iyengar, and K. Hsu, "Effect of ultrasonic vibration on interlayer adhesion in fused filament fabrication 3D printed ABS," *Polymers*, vol. 11, no. 2, p. 315, Feb. 2019, doi: 10.3390/polym11020315.

[20] R. P. Wool, B.-L. Yuan, and O. J. McGarel, "Welding of polymer interfaces," *Polymer Engineering & Science*, vol. 29, no. 19, pp. 1340–1367, 1989, doi: 10.1002/pen.760291906.

[21] Y. Yan, R. Zhang, G. Hong, and X. Yuan, "Research on the bonding of material paths in melted extrusion modeling," *Materials & Design*, vol. 21, no. 2, pp. 93–99, Apr. 2000, doi: 10.1016/S0261-3069(99)00058-8.

[22] N. Aliheidari, J. Christ, R. Tripuraneni, S. Nadimpalli, and A. Ameli, "Interlayer adhesion and fracture resistance of polymers printed through melt extrusion additive manufacturing process," *Materials & Design*, vol. 156, pp. 351–361, Oct. 2018, doi: 10.1016/j.matdes. 2018.07.001.

[23] R. H. Sanatgar, C. Campagne, and V. Nierstrasz, "Investigation of the adhesion properties of direct 3D printing of polymers and nanocomposites on textiles: Effect of FDM printing process parameters," *Applied Surface Science*, vol. 403, pp. 551–563, May 2017, doi: 10.1016/j.apsusc.2017.01.112.

[24] V. Kishore, C. Ajinjeru, A. Nycz, B. Post, J. Lindahl, V. Kunc, and C. Duty, "Infrared preheating to improve interlayer strength of big area additive manufacturing (BAAM) components," *Additive Manufacturing*, vol. 14, pp. 7–12, Mar. 2017, doi: 10.1016/j.addma. 2016.11.008.

[25] A. K. Ravi, A. Deshpande, and K. H. Hsu, "An in-process laser localized pre-deposition heating approach to inter-layer bond strengthening in extrusion based polymer additive manufacturing," *Journal of Manufacturing Processes*, vol. 24, pp. 179–185, Oct. 2016, doi: 10.1016/j.jmapro.2016.08.007.

[26] R. Mishra, W. B. Powers, and K. Kate, "Comparative study of vibration signatures of FDM 3D printers," *Progress in Additive Manufacturing*, vol. 8, no. 2, pp. 205–209, Apr. 2023, doi: 10.1007/s40964-022-00323-5.

[27] M. Kam, H. Saruhan, and A. İpekci, "Investigation the effects of 3D printer system vibrations on mechanical properties of the printed products," *Sigma Journal of Engineering and Natural Sciences*, vol. 36, pp. 655–666, Sep. 2018.

[28] I. E. Gunduz, M. S. McClain, P. Cattani, G. T.-C. Chiu, J. F. Rhoads, and S. F. Son, "3D printing of extremely viscous materials using ultrasonic vibrations," *Additive Manufacturing*, vol. 22, pp. 98–103, Aug. 2018, doi: 10.1016/j.addma.2018.04.029.

[29] P. Krishnasamy, P. C. K. Arvinda, G. J. T. Rajamurugan, A. Maniyambath, and C. J. Kesav, "Dynamic mechanical behavior of mono/synthetic-natural fiber composites—a review," *Engineering Research Express*, vol. 4, no. 4, Oct. 2022, Art. no. 042001, doi: 10.1088/2631-8695/ac9bcd.

[30] M. N. Shunmugam, S. Sankaranarayanan, N. Pandiarajan, B. K. Parrthipan, and B. Pandiarajan, "Enhancing mechanical properties of PLA filaments through orange peel powder reinforcement: Optimization of 3D printing parameters," *Applied Science and Engineering Progress*, vol. 17, no. 4, Aug. 2024, doi: 10.14416/j.asep.2024.08.011.

[31] T. Sangkharat and L. Techawinyutham, "Development of screw-based 3D printing machine and process experiments for short fiber reinforced polymer composites," *Applied Science and Engineering Progress*, vol. 17, no. 2, Nov. 2023, doi: 10.14416/j.asep.2023.11.005.